

# IDENTIFICATION OF HALO ORBITS FOR ENERGY EFFICIENT FORMATION FLYING

Oliver JUNGE\*, Jens LEVENHAGEN<sup>+</sup>, Albert SEIFRIED\* and Michael DELLNITZ\*

\*Department of Computer Science  
Electrical Engineering and Mathematics  
University of Paderborn  
33095 Paderborn Germany

<sup>+</sup>Astrium GmbH  
88039 Friedrichshafen  
Germany

**ABSTRACT** – *This contribution is concerned with the numerical simulation of spacecraft formation dynamics on Halo orbits around the Sun-Earth libration points. The circular restricted three-body problem (CRTBP) in rotating coordinates serves as the analytical framework. The primary goal is to identify regions in phase space in which the uncontrolled dynamics induces only very small perturbations on satellite formations and thus allow for an energy-optimal formation keeping strategy. This obviously leads to lower cost and mass budgets and longer operation times. The results obtained here indicate that it is possible to perform an accurate formation keeping around the libration points purely based on low thrust manoeuvres. This will be of particular importance with regard to upcoming low thrust missions such as DARWIN.*

## 1 INTRODUCTION

Halo orbits<sup>1</sup> have been identified as convenient locations for positioning single spacecraft and have already been employed for a variety of missions (e.g. NASA's GENESIS Discovery Mission). Based on the experience with these single spacecraft, also upcoming formation missions like DARWIN are foreseen to operate in the vicinity of a Halo orbit around one of the Sun-Earth libration points. This location yields the great advantage of very small gravitational disturbance forces and is therefore very well suited for missions with extremely high performance requirements. Simultaneously longer formation operation times as well as lower cost and mass budgets are guaranteed.

Concerning these missions the following important question arises: can a Halo orbit be found where a formation with several hundred meters or even kilometers of distance between the participating spacecraft could be maintained exclusively by low-thrust manoeuvres – i.e. the maximum required acceleration is in the order of or below  $10^{-9}m/s^2$ ? In that case the propellant consumption due to formation control could be neglected in comparison to that due to orbit control. In this article we present an approach which leads to the identification of Halo orbits around the  $L_2$  libration point with this desired property.

## 2 MODELLING FORMATION FLIGHT

Considering only gravitational forces, the mathematical model for the motion of several spacecraft is given by an  $n$ -body problem, i.e. by a set of coupled second order nonlinear ordinary differential equations:

$$\ddot{x}_j = G \sum_{\substack{i=1 \\ i \neq j}}^n m_i \frac{x_i - x_j}{\|x_i - x_j\|^3}, \quad j = 1, \dots, n. \quad (2.1)$$

---

<sup>1</sup> The name Halo orbit is due to the fact that it appears as a halo around the Sun when viewed from behind the Earth.

Here  $x_i \in \mathbb{R}^3$  is the position of the  $i$ -th body under consideration,  $m_i$  is its mass and  $G$  is the gravitational constant. For spacecraft dynamics this system can be significantly simplified by using the following facts: (1) the masses of the spacecraft are several orders of magnitude smaller than those of the planets and the Sun, (2) the gravitational forces between the spacecraft are negligible compared with the others, (3) up to a distance of approximately 0.01 AU from the Earth the gravitational forces of the Sun and the Earth are at least two orders of magnitude larger than those of the other planets and the Moon [Sei02]. By neglecting the corresponding force terms in (2.1) one ends up with a 3-body problem modelling the flight of each of the spacecraft separately. Further simplification of this model is achieved by restricting the motion of the Sun and the Earth to circles which leads to the well-known *circular restricted three body problem (CRTBP)*<sup>2</sup>. Its equations of motion in a rotating coordinate frame are given by [Wie98]

$$\begin{aligned}\ddot{x} &= 2\dot{y} + x + c_1(x + \mu - 1) + c_2(x + \mu) \\ \ddot{y} &= -2\dot{x} + y + (c_1 + c_2)y \\ \ddot{z} &= (c_1 + c_2)z,\end{aligned}\tag{2.2}$$

where  $(x, y, z)$  denote dimensionless coordinates with

$$c_1 = -\frac{\mu}{((x + \mu - 1)^2 + y^2 + z^2)^{\frac{3}{2}}}, \quad c_2 = -\frac{1 - \mu}{((x + \mu)^2 + y^2 + z^2)^{\frac{3}{2}}}\tag{2.3}$$

and  $\mu = m_1/(m_1 + m_2) = 3.040423398444176 \cdot 10^{-6}$  is the normalized mass of the Earth.

### 3 GENERATION OF HALO ORBITS

#### 3.1 Computation of Halo orbits

The CRTBP in rotating coordinates (2.2) has five equilibrium points, the so-called *libration* or *Lagrange points*  $L_1, \dots, L_5$ , as shown in Figure 1.

It is known [BHL97,PDD01] that there exist families of periodic orbits – the so called *Halo orbits* around the Lagrange points  $L_1$  and  $L_2$ . Our goal is to give an estimate of how costly (in terms of control acceleration) it is to control a spacecraft formation on a Halo orbit. In particular we identify those Halo orbits for which the cost is a minimum. In order to compute a family of promising Halo orbits we use a two-step path-following method as follows:

*Step 1:* To obtain an initial Halo orbit we use a *shooting* approach, see e.g. [SB80]: The Halo orbits, projected onto the three-dimensional position space, are symmetric with respect to the plane  $y = 0$ . This implies that for a point  $\mathbf{X} = (x, 0, z, \dot{x}, \dot{y}, \dot{z})$  in the vicinity of a Halo orbit in phase space we have  $\dot{x} = \dot{z} = 0$ . Prescribing one of the free remaining parameters – typically  $x$  (near  $L_2$ ) – we can thus formulate a root solving problem for the two others, namely  $z$  and  $\dot{y}$ . We solve this problem using Newton’s method and obtain initial guesses through an interval bisection method [Sei02].

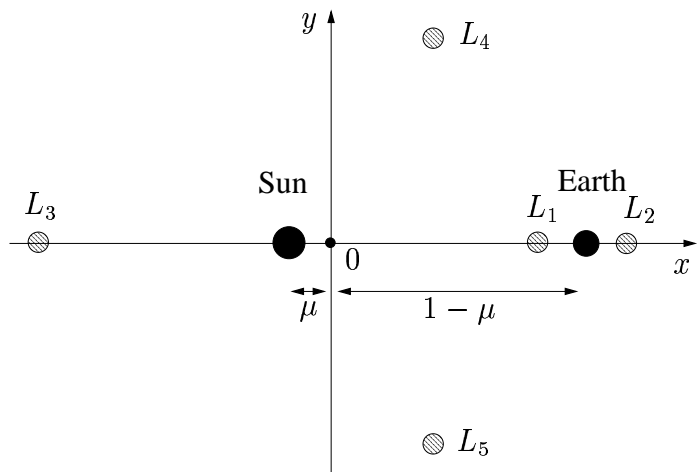


**Fig. 1:** The five Lagrange points  $L_1, \dots, L_5$  of the circular restricted three body problem.

<sup>2</sup> This problem was originally formulated by Euler in 1772.

*Step 2:* Once a Halo orbit is found for a prescribed  $x$  we get a nearby orbit of the family by a standard predictor-corrector approach: we slightly vary  $x$  in  $\mathbf{X}$  and use this point as a new initial guess for Newton's method. Figure 2 shows a family of Halo orbits around  $L_2$  which was computed by the method described. The line joining the Halo orbits marks the points  $(x, 0, z)$  which parameterise the family. In the following sections we will use the  $x$ -coordinate of these points in order to refer to a specific orbit of this family. We further refer to [TW96] for a similar approach to the computation of Halo orbits.

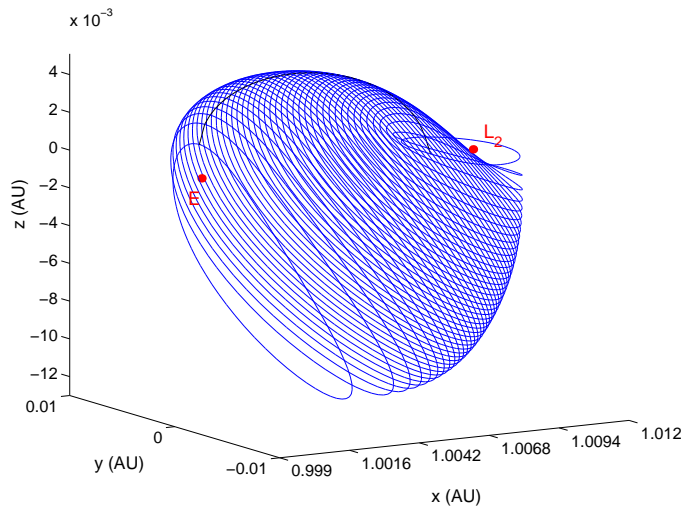


**Fig. 2:** Family of Halo orbits in the vicinity of the Lagrange point  $L_2$  (projection onto position space).

### 3.2 Stability Analysis for Halo orbits

In order to get a first impression of the dynamics in the vicinity of the Halo orbits we compute their Floquet multipliers. By definition, the Floquet multipliers of a periodic solution determine its stability [Hal80]. They are obtained via integrating the variational equation over a whole period of the corresponding periodic solution. Inspecting Figure 3 we note that there exist some orbits near the Earth for which the magnitude of all Floquet multipliers is equal to 1. Indeed, a long-time integration of these orbits indicates that they are stable. We observe that the largest Floquet-multiplier increases in magnitude as one moves along the family of Halo orbits away from the Earth. Since this multiplier determines how quickly trajectories diverge from each other, one could be tempted to argue that in order to achieve a low energy control of a formation a Halo orbit near the Earth should be selected (see also [BHL97]).

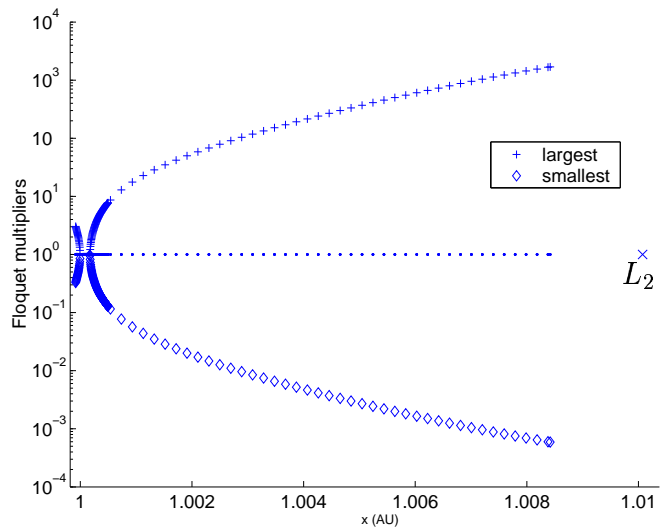


**Fig. 3:** Magnitude of the Floquet multipliers of the family of Halo orbits in Figure 2.

However, we intend to use continuously applied low thrust control on the spacecraft, thus in our case it is more interesting to obtain statements about the local dynamics on a much shorter time scale. To this end, we compute *finite time Lyapunov multipliers (FTLM)* in an analogous way as the Floquet multipliers before: but here we only integrate the variational equation for times  $\Delta t = \frac{\pi}{300}$  (which corresponds to a flight time of approximately 14 hours). See [Lor65] for the related notion of *finite time Lyapunov exponents*.

We repeat this computation along each Halo orbit and for the whole family that was computed in the previous section. The result is shown in Figure 4. We note that the maximum

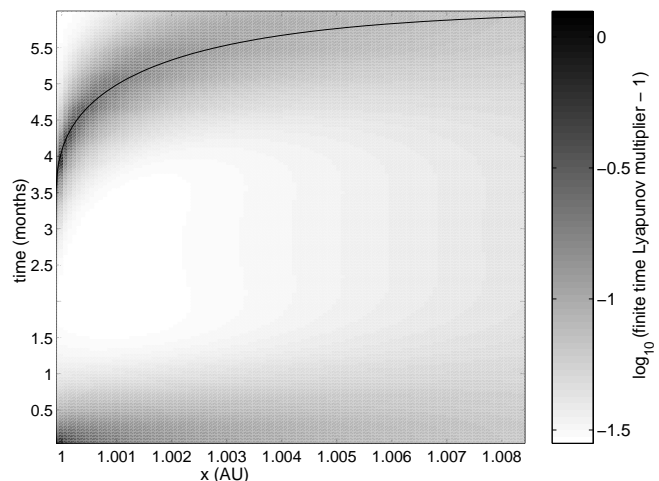


**Fig. 4:** Magnitude of the largest finite time Lyapunov multiplier (FTLM) along each Halo orbit of the family in Figure 2. The black line marks the period of the Halo orbits.

of the largest FTLM over one Halo orbit decreases when we move along the Halo orbit family away from Earth.

Since the largest FTLM determines how much a given formation of spacecraft is perturbed under the uncontrolled dynamics within the time span under consideration, one has to draw the reverse conclusion as from the results shown in Figure 3: one should **not** place the formation in the vicinity of a near Earth Halo orbit. A more detailed explanation is given in the next section.

#### 4 DEFORMATION UNDER UNCONTROLLED DYNAMICS

We analyse to what extent a given formation is deformed when evolving uncontrolled near an  $L_2$  Halo orbit. Hence we consider a particular formation, propagate each of the spacecraft using the CRTBP (2.2), and determine the time-dependent deviations of the spacecrafts' positions from the desired ones. Moreover we determine how much the *attitude of the formation* (given by the normal direction on a plane defined by the positions of the spacecraft) changes with time. This is also of particular interest in the context of missions like DARWIN.

Suppose that at time  $t_0$  an unperturbed starting formation  $F(t_0) = \{\mathbf{X}_1(t_0), \dots, \mathbf{X}_n(t_0)\}$  of  $n$  spacecraft is given, where  $\mathbf{X}_j(t_0) = (\mathbf{X}_j^q(t_0), \mathbf{X}_j^p(t_0)) \in \mathbb{R}^6$  denote the dimensionless locations in phase space ( $\mathbf{X}_j^q(t_0)$  names the position,  $\mathbf{X}_j^p(t_0)$  the velocity of the  $j$ -th spacecraft). We denote by  $\mathbf{X}(t; \mathbf{X}_j(t_0))$  the solution of (2.2) for the initial value  $\mathbf{X}_j(t_0)$ . In this paper we restrict ourselves to formations of  $n = 4$  spacecraft arranged as a regular tetrahedron (see Figure 5). Hence initially (i.e. for  $t = t_0$ ) we require that  $\|\mathbf{X}_j^q(t_0) - \mathbf{X}_k^q(t_0)\| = c = \text{const}$  for all  $j \neq k$ . Moreover, we make use of the fact that we are interested in the *relative* positions of the spacecraft with respect to each other – and also that all our computations involve only short-time integration (approximately 14 hours, see Section 3.2) of the underlying differential equation. We thus perform our calculations in a *local coordinate system*, using the variational equation corresponding to (2.2) for time integration.<sup>3</sup>

In order to analyse the deformation of the tetrahedral formations under their uncontrolled dynamics in the neighborhood of a Halo orbit, we first consider a prescribed tetrahedron with its geometric centre in the origin, i.e. four points  $\{\mathbf{X}_1^q, \dots, \mathbf{X}_4^q\} \subset \mathbb{R}^3$  with

$$\frac{1}{4} \sum_{j=1}^4 \mathbf{X}_j^q = 0. \quad (4.1)$$

We use this tetrahedron in order to derive initial formations along a Halo orbit, which are evolved afterwards using the CRTBP (2.2). To this end, we first choose a set of points  $\mathbf{M}_i = (\mathbf{M}_i^q, \mathbf{M}_i^p) \in \mathbb{R}^6$ ,  $i = 1, \dots, \ell$ , on some Halo orbit. These points serve as the geometric centers of the initial formations. From these points we derive formations as follows: For each of these points we consider the formation  $F_i(t_0) = \{\mathbf{X}_{i,1}(t_0), \dots, \mathbf{X}_{i,4}(t_0)\}$ , where  $\mathbf{X}_{i,j}(t_0) = (\mathbf{X}_{i,j}^q(t_0), \mathbf{X}_{i,j}^p(t_0))$ , defined by

$$\mathbf{X}_{i,j}^q(t_0) = \mathbf{R}_i \mathbf{X}_j^q + \mathbf{M}_i^q \quad \text{and} \quad \mathbf{X}_{i,j}^p(t_0) = \mathbf{M}_i^p, \quad j = 1, \dots, 4. \quad (4.2)$$

Here  $\mathbf{R}_i \in \mathbb{R}^{3 \times 3}$  is the matrix describing a rotation about the local  $z$ -axis by some angle  $\theta_i$ . This rotation is compensating for the fact that the CRTBP is formulated in a rotating coordinate system,

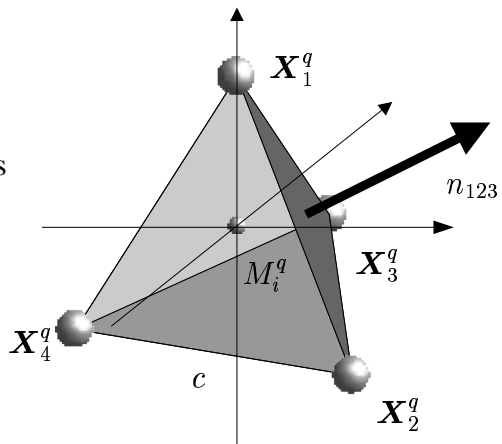


Fig. 5: Formation of four spacecraft arranged as a regular tetrahedron.

<sup>3</sup> We also note that the scales of interest to us differ by a factor of  $10^{13}$ : the distance between the Sun and the Earth is of the order of  $10^{11}$  m and we hold the spacecraft relative to each other within an error bound of about 0.01 m. Using the standard double-precision floating point arithmetic rounding errors will notably influence any corresponding computation.

but – in view of missions like DARWIN – we want the formation to maintain an inertially fixed orientation. So in (4.2) we first rotate the tetrahedron  $\{\mathbf{X}_1^q, \dots, \mathbf{X}_4^q\}$ , such that we obtain the correct attitude and then move it onto the Halo orbit such that its geometric center is  $\mathbf{M}_i^q$  afterwards.

The sum of differences between actual and desired edge lengths

$$D_i(t) = \sum_{j=1}^{n-1} \sum_{k=j+1}^n \left| \frac{\|\mathbf{X}_{i,j}^q(t) - \mathbf{X}_{i,k}^q(t)\|}{\|\mathbf{X}_{i,j}^q(t_0) - \mathbf{X}_{i,k}^q(t_0)\|} - 1 \right| \quad (4.3)$$

is a measure for the *deformation* of the formation  $F_i(t)$ . Here we abbreviated notation by writing  $\mathbf{X}_{i,j}^q(t)$  for the position space coordinates of the solution  $\mathbf{X}(t; \mathbf{X}_{i,j}(t_0))$ . In order to attribute a specific direction to a formation  $F_i(t) = \{\mathbf{X}_{i,1}(t), \dots, \mathbf{X}_{i,4}(t)\}$ , we choose three spacecraft  $\mathbf{X}_{i,1}(t)$ ,  $\mathbf{X}_{i,2}(t)$  and  $\mathbf{X}_{i,3}(t)$  from  $F_i(t)$  and define the *attitude* of  $F_i(t)$  by the accompanying plane unit normal vector

$$\mathbf{n}_i(t) = \frac{(\mathbf{X}_{i,2}^q(t) - \mathbf{X}_{i,1}^q(t)) \times (\mathbf{X}_{i,3}^q(t) - \mathbf{X}_{i,1}^q(t))}{\|(\mathbf{X}_{i,2}^q(t) - \mathbf{X}_{i,1}^q(t)) \times (\mathbf{X}_{i,3}^q(t) - \mathbf{X}_{i,1}^q(t))\|}. \quad (4.4)$$

Based on this approach one can define the *tilt angle* of the formation at time  $t$  as

$$\alpha_i(t) = \arccos(\mathbf{n}_i(t_0) \cdot \mathbf{n}_i(t)). \quad (4.5)$$

*Example:* In the following computations we use an edge length of 433 m between the four spacecraft. We use a set of  $\ell = 300$  points on the Halo orbit that we obtained by integrating along the orbit for periods  $\Delta t = \frac{\pi}{300}$ . (Here  $2\pi$  corresponds to one year; the Halo orbits have periods between 4 and 6 months.) For this  $\Delta t$  and for every  $i = 1, \dots, \ell$  the deformation  $D_i(t_0 + \Delta t)$  and the tilt angle  $\alpha_i(t_0 + \Delta t)$  are computed. Figure 6 shows the result for an initial tetrahedron with a randomly chosen attitude on the Halo orbit through the point  $\mathbf{X} = (1.0057, 0, 0.0044, 0, 0.0179, 0)$  with a period of approximately 177 days. We note that though we have chosen the attitude of the initial tetrahedron at random, the result is representative in the sense that different initial tetrahedra lead to comparable results.

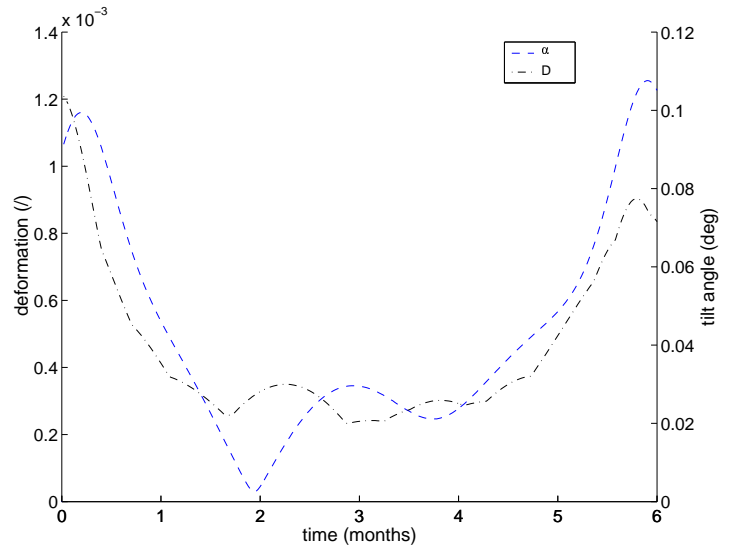
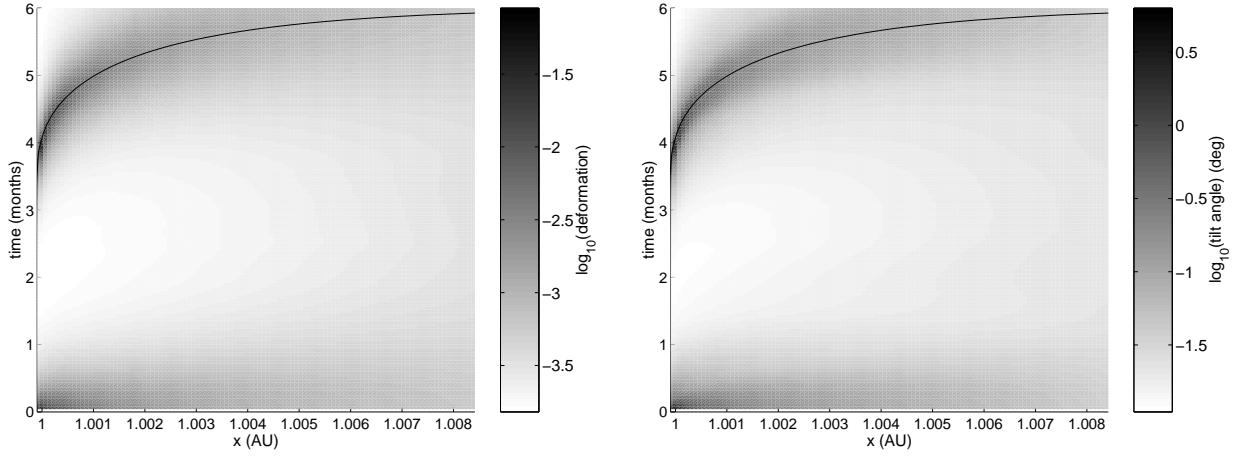


Fig. 6: Deformation/tilt angle of a spacecraft formation along an  $L_2$  Halo orbit.

we note that though we have chosen the attitude of the initial tetrahedron at random, the result is representative in the sense that different initial tetrahedra lead to comparable results.

This computation is performed for the entire family of Halo orbits of Section 3 where, in addition, we average the result for each Halo orbit over 100 initial tetrahedra with randomly chosen attitude. The results are shown in Figure 7. The abscissa parameterises the family of orbits and the ordinate represents time, i.e. parameterises the set of points  $\mathbf{M}_i$ . The shading indicates the deformation (left subplot) and the tilt angle of the formation (right subplot) in a logarithmic scale, respectively. Note that these two figures closely resemble Figure 4.

In Figure 8 the two quantities are displayed in a different way. This time their minimum, maximum and mean values over each of the Halo orbits of the family are shown, respectively. Observe that the mean deformation exhibits a local minimum at approximately  $x = 1.0065$  (see Figure 8 (left)). However, for practical purposes the existence of this minimum is of minor importance. Rather we observe that the mean and the maximum deformation and tilt angle of a formation under uncontrolled dynamics along a Halo orbit essentially decreases when we move along the family of Halo orbits away from the Earth. Thus we draw the conclusion that Halo orbits further away from the Earth are



**Fig. 7.** Deformation (left) and tilt angle (right) of a spacecraft formation along the  $L_2$  Halo orbit family from Figure 2. The black lines mark the period of the Halo orbits.

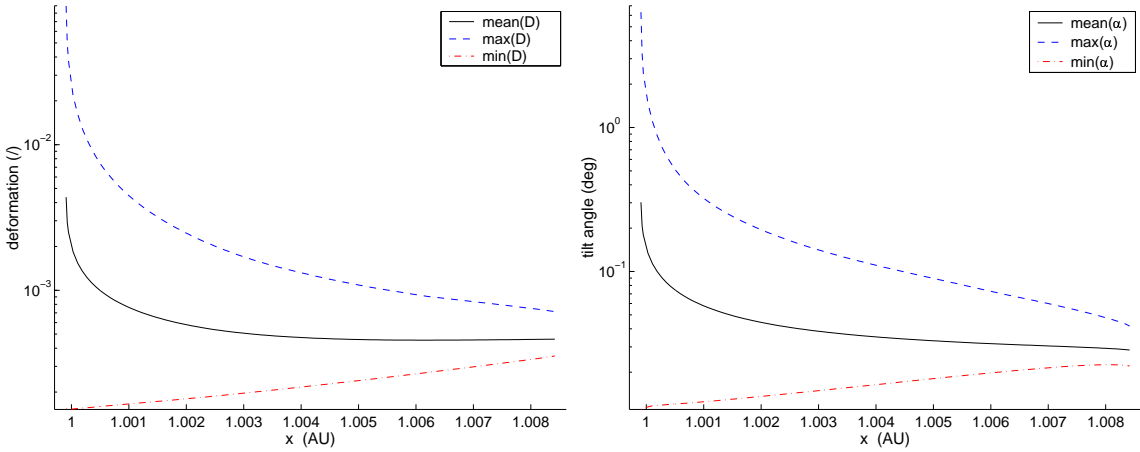


**Fig. 8.** Minimum, maximum and mean deformation (left) and tilt angle (right) of a spacecraft formation along the  $L_2$  Halo orbit family from Figure 2.

better suited for an energy efficient formation flight (which obviously confirms our interpretation of Section 3.2). In the next section we will see that this conclusion is further supported when a controlled flight of spacecraft is considered.

## 5 LOW THRUST CONTROL STRATEGY

This section complements the results of the previous sections with the analysis of a certain control strategy for stabilizing the spacecraft formation on an  $L_2$  Halo orbit. Our approach is as follows: We add control acceleration terms  $\mathbf{u} = (u_x, u_y, u_z)$  to equation (2.2), yielding the system

$$\begin{aligned}
 \ddot{x} &= 2\dot{y} + x + c_1(x + \mu - 1) + c_2(x + \mu) + u_x \\
 \ddot{y} &= -2\dot{x} + y + (c_1 + c_2)y + u_y \\
 \ddot{z} &= (c_1 + c_2)z + u_z.
 \end{aligned} \tag{5.1}$$

The solution of (5.1) will thus depend on the *control function*  $\mathbf{u} = \mathbf{u}(t)$ , i.e. starting in  $\mathbf{X}(t_0)$  and applying the control function  $\mathbf{u}$  one arrives at  $\mathbf{X}(t; \mathbf{u}, \mathbf{X}(t_0))$ . We can now formulate our control problem as follows: given some actual formation  $F_t = \{\mathbf{X}_1(t), \dots, \mathbf{X}_n(t)\}$  at each time instance  $t$

and a prescribed reference formation  $F_{t+\Delta t} = \{\mathbf{X}_1(t + \Delta t), \dots, \mathbf{X}_n(t + \Delta t)\}$  at  $t + \Delta t$ , find control functions  $\mathbf{u}_j = \mathbf{u}_j(t)$ , such that

$$\mathbf{X}(\Delta t; \mathbf{u}_j, \mathbf{X}_j(t)) = \mathbf{X}_j(t + \Delta t) \quad \text{for } j = 1, \dots, n. \quad (5.2)$$

Motivated by physical considerations (i.e. the design of the spacecraft thrusters) we make the assumption, that the control functions  $\mathbf{u}_j(t)$  are piecewise constant. If we restrict ourselves to two “time steps” per period  $\Delta t$  (i.e.  $\mathbf{u}_j(t)$  is constant on  $[t, t + \Delta t/2]$  and constant but eventually different on  $[t + \Delta t/2, t + \Delta t]$ ), equation (5.2) yields a system of six equations and six unknowns. If we choose  $\Delta t$  sufficiently small and if the actual formation is “sufficiently close” to the reference formation, we can solve this system using Newton’s method.

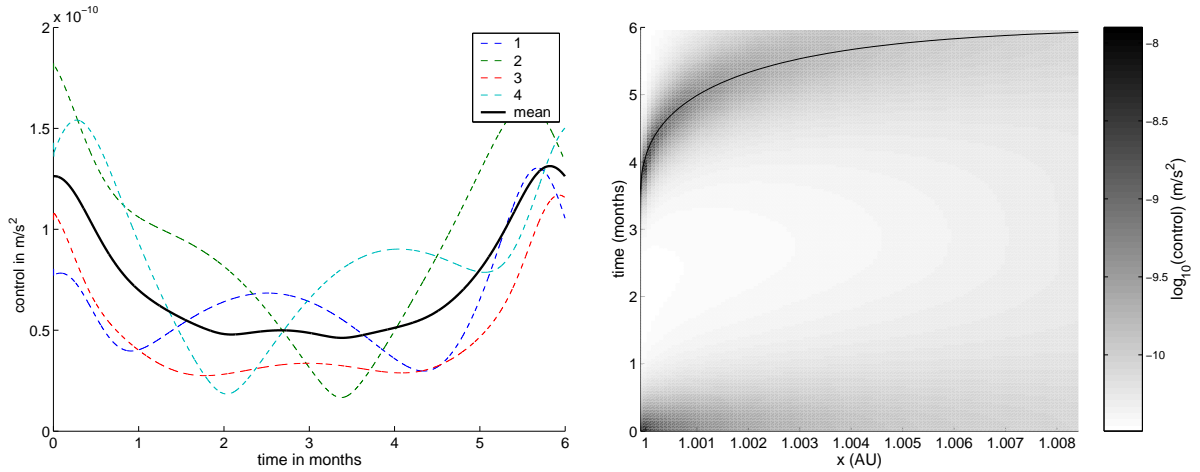


**Fig. 9.** Left: Magnitude of the control acceleration (for each spacecraft separately and their mean) along some Halo orbit. Right: Magnitude of control acceleration along the Halo orbit family of Figure 2.

Figure 9 (left) shows the magnitude of the required control acceleration in dependence of time along a certain Halo orbit (the one we used in Section 4). Note the qualitative similarity to Figure 6. We repeat the same computation for the whole family of Halo orbits and average the results over 50 randomly chosen reference formations. The result is shown in Figure 9 (right). As expected it bears a strong resemblance with Figures 4 and 7.

In Figure 10 we plot the minimum, maximum and the mean control acceleration along the Halo orbit family. Again, these values show the same dependence as the deformation which has been computed in the previous section (Figure 8). But more important is the fact that Halo orbits can be identified with a required maximum control acceleration below  $10^{-9} \text{ m/s}^2$  which makes it possible to keep the vehicles in a stable formation only by low thrust actuation.

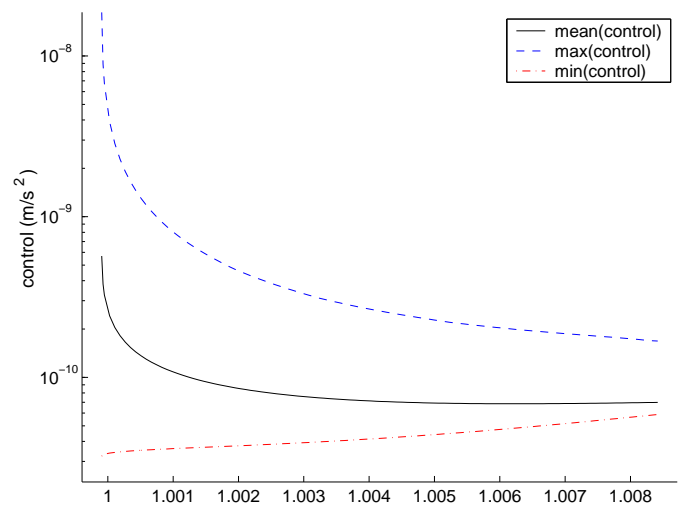


**Fig. 10:** Minimum, maximum and mean (over one period) control acceleration along that family.

## 6 DISCUSSION

Based on the CRTBP given in a rotating coordinate frame, we present an approach to identify Halo orbits around  $L_2$  which are suitable locations for an energy efficient formation flight. Within that context the evaluation of *finite time Lyapunov multipliers* indicates that promising Halo orbits are located at some distance from the Earth. A detailed analysis of the dynamical behaviour of uncontrolled as well as controlled formations verifies this important result.

In all the computations we use formations of four spacecraft arranged as a tetrahedron in the vicinity of Halo orbits around  $L_2$ . Energy efficiency is derived from two local deformation measures and a simple but straightforward control strategy is employed. The results obtained contradict the conclusions which one might draw from ordinary Floquet multipliers analysis.

As a very important result it is shown that a lifetime formation control only based on low thrust actuation is possible. Regarding future mission design, this will allow to neglect propellant consumption due to formation control compared to that due to orbit control. However, the propellant needed for the *reconfiguration* of a formation is not taken into account and will be a topic of our future work.

## References

- [BHL97] B.T. Barden, K.C. Howell, and M.W. Lo. Application of dynamical systems theory to trajectory design for a libration point mission. *J. of the Astronautical Sciences*, 45(2):161–178, 1997.
- [Hal80] J.K. Hale. *Ordinary differential equations*. Wiley-Interscience, 1980.
- [Lor65] E.N. Lorenz. A study of the predictability of a 28-variable atmospheric model. *Tellus*, 17:321–333, 1965.
- [PDD01] R.C. Paffenroth, E.J. Doedel, and D.J. Dichmann. Continuation of periodic orbits around Lagrange points and AUTO2000. In *Proc. AAS/AIAA Astrodynamics Specialist Conference*, 2001. AAS paper 01-303.
- [SB80] J. Stoer and R. Bulirsch. *Introduction to numerical analysis*. Springer, 1980.
- [Sei02] A. Seifried. Numerische Untersuchungen zum Formationsflug von Raumfahrzeugen. Diploma thesis, Universität Paderborn, 2002. To be published.
- [TW96] R. Thurman and P.A. Worfolk. The geometry of halo orbits in the circular restricted three body problem. Technical Report GCG95, Geometry Center, University of Minnesota, 1996.
- [Wie98] B. Wie. *Space Vehicle Dynamics and Control*. AIAA Education Series. AIAA, 1998.